MICROSTRUCTURAL AND GEOMECHANICAL CHARACTERISATION OF FAULT ROCKS FROM THE CARNARVON AND OTWAY BASINS

D.N. Dewhurst[1], R.M. Jones[2], R.R. Hillis[3] and S.D. Mildren[3]
[1]CSIRO Petroleum
Australian Petroleum Cooperative Research Centre
ARRC, 26 Dick Perry Avenue
Technology Park
Kensington WA 6151
[2]Woodside Energy Ltd
1 Adelaide Terrace
Perth WA 6000
[3]National Centre for Petroleum Geology and Geophysics
Australian Petroleum Cooperative Research Centre
Adelaide University
Thebarton Campus
Adelaide SA 5005

ABSTRACT

The results of natural and laboratory-induced fault behaviour from wells in the Otway Basin are compared with sample material from a producing Carnarvon Basin field where rocks from a fault zone have been cored. Capillary pressure, microstructural and juxtaposition data obtained from these fault rocks indicate a capability to hold back gas columns in excess of 100 m, yet many fault closures are found to contain only palaeo-columns. Trap failure is usually attributed to reactivation of trap-bounding faults, often during Miocene-Recent times in these basins. Faults susceptible to reactivation can be predicted by geomechanical methods involving the determination of the in-situ stress field and the orientation and dip of faults with respect to that stress field. Failure envelopes of fault rocks have been determined to estimate reactivation potential in the present day in-situ stress field. This approach works well where fault rocks are weaker than the host reservoir sandstone, but may not be applicable where fault rocks are stronger. In fields where the latter is the case, intact hydrocarbon columns are present, irrespective of whether faults are optimally oriented for reactivation. This indicates that the assumptions of zero cohesive strength and constant friction coefficient for predicting the reactivation potential of fault rocks may not be completely reliable.

KEYWORDS

Fault seal prediction, geomechanics, fault rocks, microstructure, capillary properties, reactivation.

INTRODUCTION

Fault sealing is recognised to be one of the major influences on hydrocarbon migration. However, few data have been published on physical properties, geomechanical properties or microstructural evolution of fault rocks in relation to hydrocarbon reservoirs. Fault seals can exhibit a wide range of lithification states, which can result in highly variable geomechanical properties, even within the damage zones of individual faults. The strength of fault-rocks governs the change in flow properties that results from changes in stress conditions within a reservoir. The development of fault zones as seals and the resultant change in host rock properties can be assessed using structural core logging, microstructural and physical property characterisation, combined with well data, seismic and outcrop studies. An important element of this approach is microstructural characterisation of different types of fault rocks present in an area.

Fault zones comprise clusters of features that form a deformation halo to large offset faults. The presence of arrays of deformational features, rather than a single fault, can influence the changes in cross-/along-fault communication induced by reactivation events. The size of a damage zone is lithology dependent, as well as being contingent on deformational conditions and the distribution of strain between the hanging wall and footwall. Research at core scale to microscale has led to an understanding of the processes that result in fault rock development (e.g. Aydin, 1978; Aydin and Johnsen, 1983; Hippler, 1997; Fisher and Knipe, 1998; Gibson, 1998). These microscale developments have allowed the categorisation of fault rocks dependent on mineralogy and have led to increased knowledge of likely sealing properties and processes in given geological situations. Clay smears form where ductile shales are entrained within a fault zone. Cemented cataclasites generally form in clean sandstones at depths >3 km. At these depths, stresses are high enough for grain fracturing to create clean surface areas; temperatures exceeding 90°C result in high silica mobility and preferential cementation (Fisher and Knipe, 1998). Phyllosilicate framework fault rocks from in impure sandstones (15–40% clay) through shear-induced mixing of clays and rigid grains (Fisher and Knipe, 1998). Well constrained lithological and juxtaposition data, tied to seismically observable fault zones can provide good estimates of seal potential along faults and suggest regions along a fault zone where potential leak windows are likely to exist. However, while such analyses can define the sealing potential of faults that have been inactive since hydrocarbon charge, they cannot incorporate the potential for seal breach due to fault reactivation subsequent to charge.

GEOMECHANICAL PROCESSES AND REACTIVATION

The lack of geomechanical data for naturally occurring intact fault rocks is a critical limiting factor in assessing the likelihood of fault seal reactivation. While there are considerable amounts of data available for geomechanical properties of cohesionless or clay-rich gouges (e.g. Morrow et al, 1982) and peak strength determinations for cataclasites from fault zones (Chester and Logan, 1986), very little data exists documenting failure conditions for intact fault rocks.

Tectonic faults relate to the localised stress regime in the basin in which they developed, and usually display systematic orientations. This may include basement reactivation resulting in faulting in the overlying sedimentary strata. As such, faults can cut sediments in different lithification states along their length and, therefore, deformation mechanisms, fault rock products and geomechanical properties may vary accordingly (Sverdrup and Bjørlykke, 1997). Fault rock texture and structure are a product of factors such as strain rate, principal stress orientation, shear sense, pore pressure, lithification state and diagenesis. Since mechanical properties change between cohesionless, unlithified sand and brittle cemented sandstones, deformation processes and fault rock products also change. Therefore, it is essential to establish the diagenetic history as well as the burial depth at which the deformation occurred in order to predict fault rock properties and their effects on fluid flow (Sverdrup and Bjørlykke, 1997). Hence both microstructural and geomechanical studies play a significant role in fault seal analysis.

Hydrocarbon traps associated with active faults and fractures are riskier than those associated with inactive faults because of the potential for fault-valve activity (Sibson, 1992). There is abundant evidence that critically stressed faults and fractures provide high permeability conduits for fluid-flow (e.g. Sibson, 1994; Muir Wood, 1994). Reactivation can breach fault-bound traps even if there is juxtaposition- and/or fault damage-related seal. The likelihood of reactivation can be assessed given knowledge of the stress field, fault orientation and the failure envelope for the fault rocks. The relationship between these variables also dictates the likely mode of failure the fault will undergo. The development of cohesive strength through fault healing allows fault rocks to fail by tensile, shear or mixed mode fracturing. Assuming faults are cohesionless allows failure in shear alone. A number of recent studies of the relationship between stresses and fault reactivation/permeability (e.g. Barton et al, 1995; Morris et al, 1996; Castillo et al, 2000; Wiprut and Zoback, 2000) assume that the failure envelopes for fault rocks are described by a cohesionless Byerlee-type friction law (Byerlee, 1978). However, frictional sliding experiments on cohesionless joints or saw-cuts through rocks of the type summarised by Byerlee (1978) do not describe the failure envelopes for fault zones such as cemented cataclasites which may exhibit significant cohesive strength.

This paper presents failure envelopes for microstructurally and petrophysically characterised fault rocks sourced intact from cores in the Carnarvon and Otway Basins of Australia. Further, given that cohesionless friction relations do not describe the failure of these fault rocks, an alternative approach to assessing the risk of fault reactivation and associated seal breach is presented and applied to a case study in the Otway Basin. We also consider a scenario from the Carnarvon Basin where the fault rock is considerably stronger than the surrounding reservoir sandstone.

METHODOLOGY

The fault rocks used in this study were sourced intact from cores recovered from the offshore Carnarvon Basin (Yodel–2, top Triassic Sandstone) and the Penola Trough, Otway Basin (Jacaranda Ridge–1 and Banyula–1, Pretty Hill Sandstone). Microstructural and petrophysical characterisation was performed on samples from all wells and geomechanical testing on a variety of fault rock types from each well. Techniques used comprise the following:

Scanning Electron Microscopy

Scanning Electron Microscopic (SEM) examination of the microstructure of the fault rocks and associated reservoir sandstones was performed on resin-impregnated polished blocks on a JEOL 25S SEM equipped with secondary electron detector, solid state 4 quadrant backscattered electron detector, Eumex Si (Li) Moxtek UTW EDS with digital image capture. All images are presented with the micrograph upper edge aligned with the top of the core.

Mercury injection porosimetry

Capillary pressure analysis was conducted using a Micromeritics Autopore III mercury porosimeter. This equipment is capable of injecting mercury in user-defined pressure increments up to 60,000 psi (~413 MPa) into a cleaned, dry sample. Directional injection across the fault seals was ensured through resin-sealing of samples on five sides and allowing footwall injection perpendicular to the fault gouge. Hydrocarbon-brine interfacial tension, density of formation water and hydrocarbon phases under sub-surface conditions were calculated via manipulation of industry standard nomographs (Schowalter, 1979).

Geomechanical testing

Samples of 50 mm length and 25 mm diameter were deformed undrained in a standard triaxial cell with full independent control of cell pressure, pore pressure and axial load. Samples were fully saturated with light oil to avoid damaging clays. Due to the small amounts of samples available, multi-stage triaxial tests were run (Fjaer et al, 1992). Samples were deformed to within a few MPa of peak strength (5–10%) at a set confining pressure then unloaded. Confining pressure was then increased followed by further application of axial load until again close to failure. This cycle was repeated until the desired number of steps had been reached. The final cycle was then taken through to failure and residual strength. Cores of both fault rocks and associated reservoir sandstones were tested for comparative purposes. Where damage zone faults or deformation features were present as single strands, they were oriented at 30° to σ_1 in the triaxial rig, in the optimum orientation for failure.

OTWAY BASIN MICROSTRUCTURAL AND POROSIMETRY RESULTS

The Mesozoic-Cenozoic Otway Basin is a passive margin basin in eastern South Australia/western Victoria/ Tasmania and is one of the most actively explored basins on the southern margin of Australia. Over the last decade, commercial gas discoveries have been made in the Katnook, Ladbroke Grove and Haselgrove Fields in the Penola Trough in the South Australian portion of the Otway Basin (Fig. 1). In that time, improvements in seismic quality, stratigraphic modelling and additional well control have greatly enhanced regional prospectivity (Willink and Lovibond, 2001) and recently led to several significant onshore and offshore discoveries in the Victorian sector of the basin and an important new gas field in Tasmanian waters.

The stratigraphy of the Penola Trough is dominated by syn-rift sediments belonging to the Lower Cretaceous Crayfish Group (Kopsen and Scholefield, 1990; Lovibond et al, 1995). These include the major reservoir sandstones of the Pretty Hill Formation and Sawpit Sandstone and the local seals of the Laira Formation and Upper Sawpit Shale. The local seal for Pretty Hill reservoirs is the Laira Formation, which was deposited in a lacustrine to delta fringe environment and comprises a series of interbedded claystones, siltstones and well-sorted lithic sandstone with argillaceous or calcareous cement. The Sawpit Shale is the local seal for the Sawpit Sandstone and is similar in lithology to the Laira Formation. All prospects containing Crayfish Group reservoirs were generated by faulting directly related to oblique syn-depositional rifting of the Penola Trough.

The principal deformation process in clean (<15% clay) Crayfish Group reservoir strata is cataclasis (Jones et al, 2000), coupled with post-deformation lithification. Maximum gas column heights able to be supported by such faults are approximately 102 m (Jones et al, 2000). Given the complex tectonic history of the region, hydrocarbon leakage due to reactivation is perhaps the major risk for fault bound traps in the Penola Trough. Indeed, natural open fractures have been identified crosscutting fault gouges within Crayfish Group reservoirs (Jones et al, 2000). These fractures will provide relatively high permeability pathways across fault seals and their existence may, in part, provide an explanation as to the existence of palaeo-hydrocarbon columns where leakage has not been due to capillary breakthrough. The integration of data on the geomechanical properties of rocks with predictive fault seal tools such as F.A.S.T. (Jones et al, 2000) reduces the uncertainty associated with the likelihood of fault seal breaching through the development of structural permeability networks.

Otway Basin fault rocks analysed as part of this study include cemented cataclasites and phyllosilicate framework fault rocks. Both fault rock types are hosted within competent medium to fine-grained cemented sandstones. The rocks have been recovered from Jacaranda Ridge–1 within a field that contains an intact hydrocarbon accumulation and from Banyula–1, a dry hole drilled off structure. The results from the latter well have been incorporated in to a model to explain the breached hydrocarbon accumulation in the Zema fault block, assuming that the geomechanical properties of the fault rocks in the Pretty Hill Sandstone at Banyula–1 are similar to those at Zema–1.

A variety of cemented and cataclastic microfaults from Jacaranda Ridge–1 are illustrated in Figure 2. Figures 2a and 2b show hand specimens of parallel trending and conjugate sets of cemented microfaults 1–2 mm wide with spacings in the order of 1–4 cm. Figure 2c illustrates extensional microfaults in a more argillaceous facies with evidence of clay entrainment into the fault gouge. SEM analysis of the reservoir microstructure reveals that extensive cementation occludes the majority of pores (Figures 2d–f). Fault identification and displacement magnitudes can be determined from the disruption of organic laminae and by the entrainment of ankerite into fault zones. Displacement is typically 1–2 mm. Ankerite can form early in the diagenetic sequence (Deer et al, 1966) and its inclusion within fault gouge, together with a lack of grain fracturing, suggests deformation occurred early in the reservoir burial history (whilst sediments were relatively unlithified). Figures 2g and 2h show a phyllosilicate framework fault rock sampled from the same damage zone in Jacaranda Ridge–1. The core contains numerous sub-parallel anastomosing seams of phyllosilicates that isolate pods of deformed and undeformed sandstone. Porosity in the sandstone is completely occluded by clays, fracturing of quartz grains is evident and clays line boundaries between more rigid grains.

Fracturing of feldspars is observed in the reservoir sandstone from Banyula–1 (Fig. 3a). However, most quartz grains remain undeformed. Diffusive mass transfer resulting from the diagenetic history of the sandstone is also evident in the form of inter-penetrating grains and embayed grain boundaries. Original cataclasite from this well appears as fine-grained fractured quartz particles contained within quartz cement (Fig. 3b). After reactivation, the microstructure is characterised by a

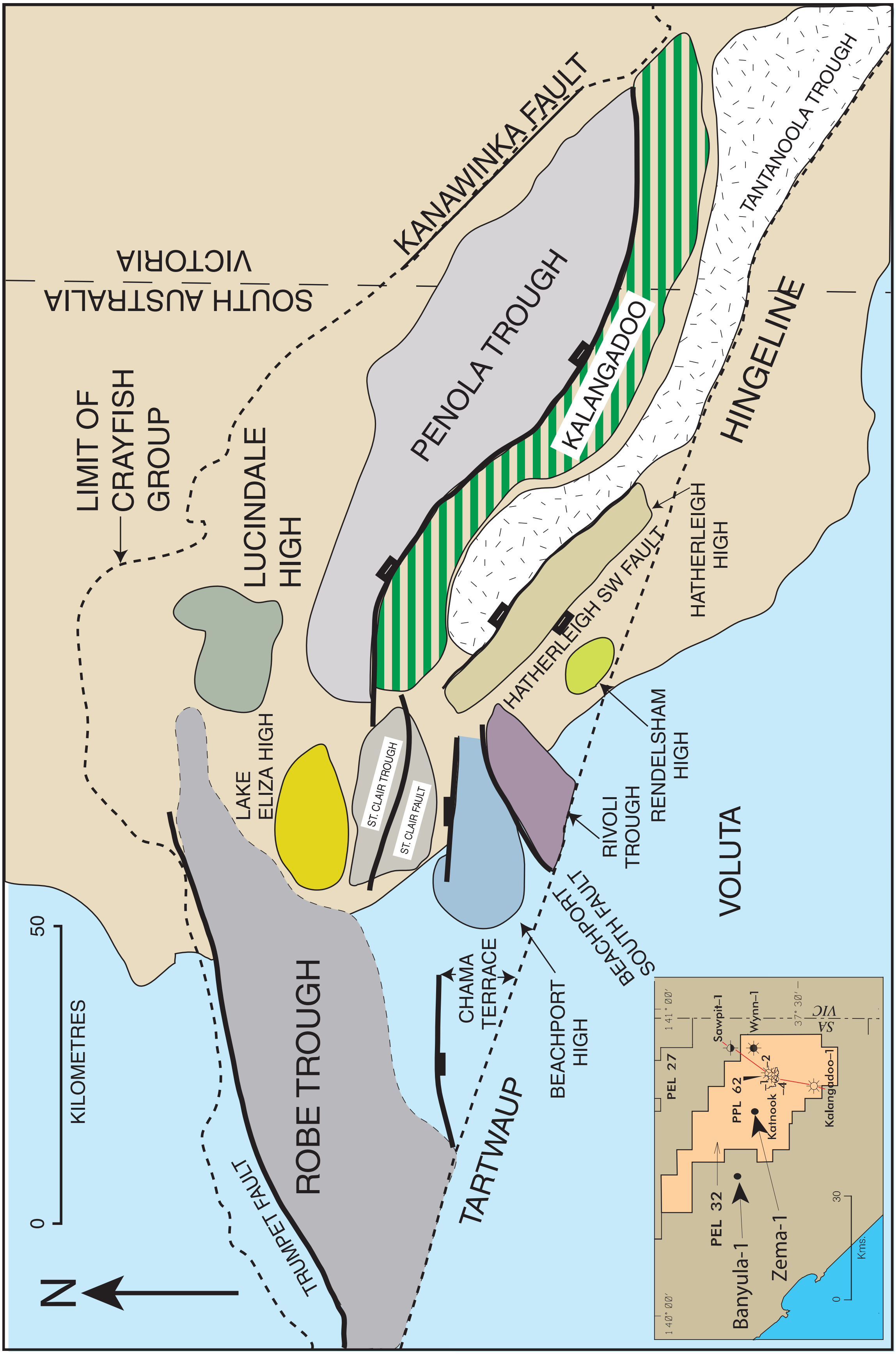

Figure 1. Location map showing the Penola Trough and wells referred to in the text.

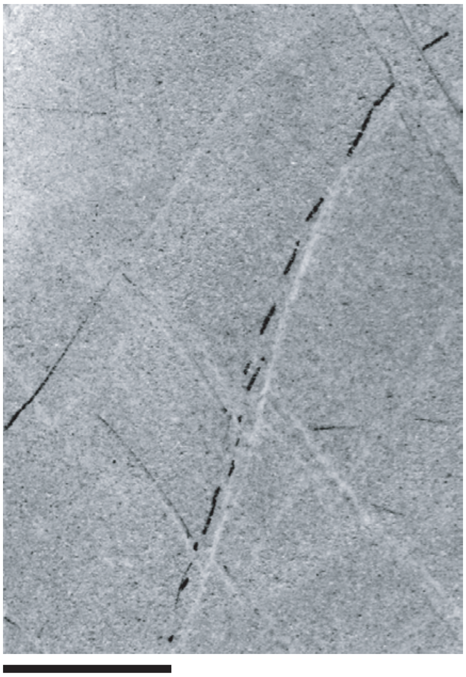

2 cm

Figure 2a. Cemented conjugate faults in a core from the Otway Basin.

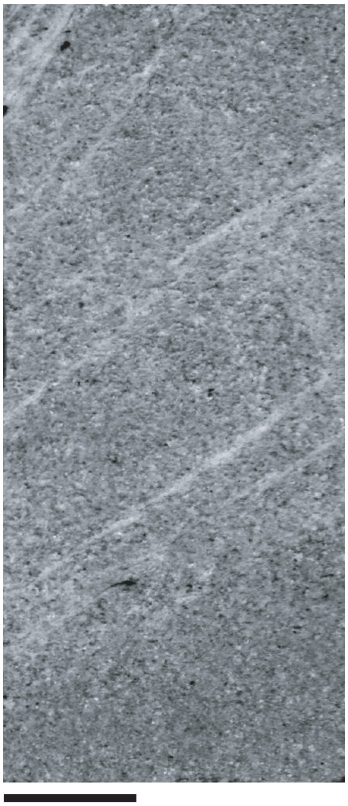

1 cm

Figure 2b. Parallel trending cemented microfaults from Jacaranda Ridge–1. The SEM images in Figs 2d–2f come from this sample.

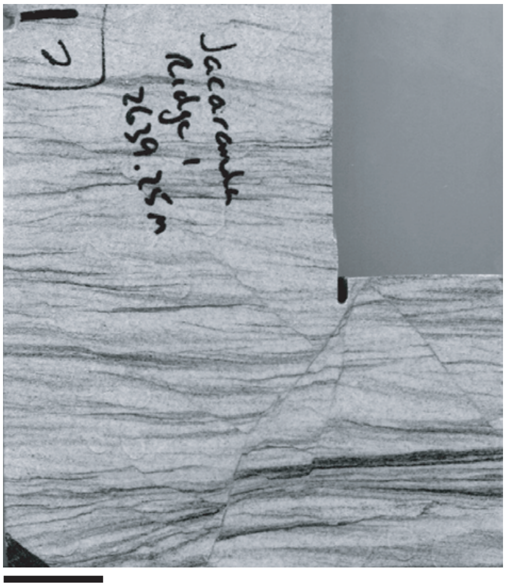

2 cm

Figure 2c. Cemented microfaults in a more argillaceous lithology in a core from Jacaranda Ridge–1 about 3 m below (a) and (b). Note drag and smearing of argillaceous laminae into fault planes.

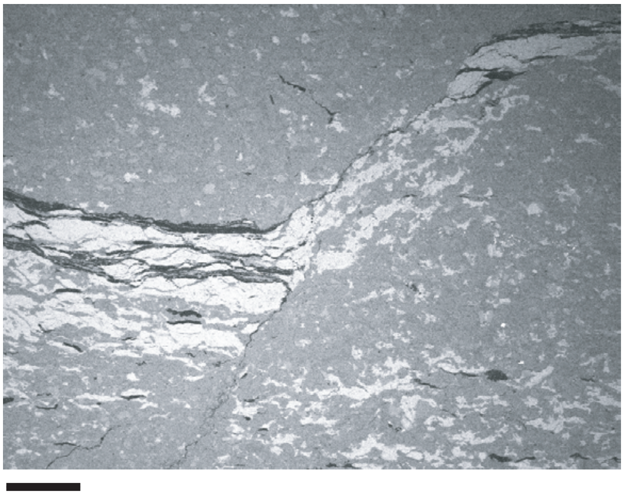

0.5 mm

Figure 2d. SEM micrograph of cemented damage zone rock from Jacaranda Ridge–1. The microfault is highlighted by dragged ankerite (light) and organic laminae (dark) suggesting early ankerite formation.

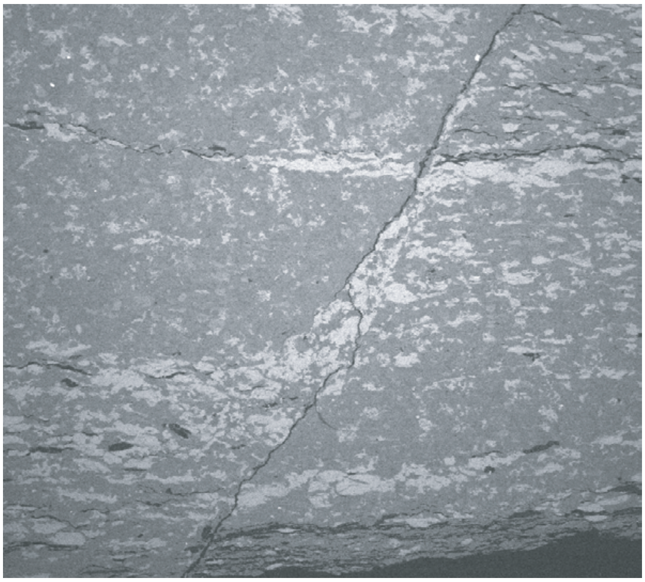

0.5 mm

Figure 2e. Laminae of organic matter and ankerite terminate at, and are dragged into, a fault zone. The rock has been heavily cemented post-deformation.

0.5 mm

Figure 2f (above). Oriented ankerite within fault zone and terminations of organic matter and ankerite laminae against the fault from core in Jacaranda Ridge–1.

Figure 2h (bottom right). Backscattered SEM image of the phyllosilicate framework fault rock, showing clays occluding pores and between quartz grains, which may have facilitated diffusive mass transfer and cementation processes in this rock.

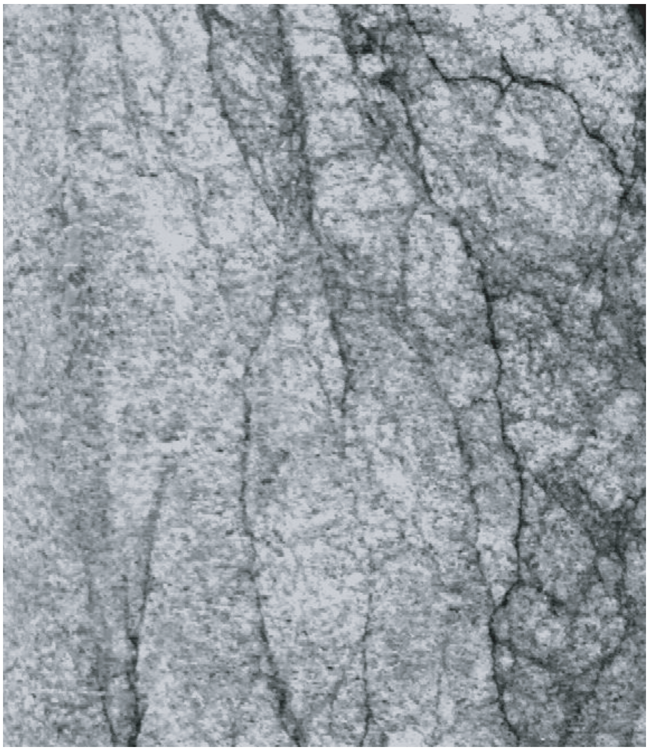

2 cm

Figure 2g. Phyllosilicate framework fault rock in core from Jacaranda Ridge–1 comprising anastomosing clay-rich seams in deformed and heavily cemented impure sandstone. This fault rock is from the same damage zone as the other faults in this figure and shows how lithological variations can influence resulting fault rocks.

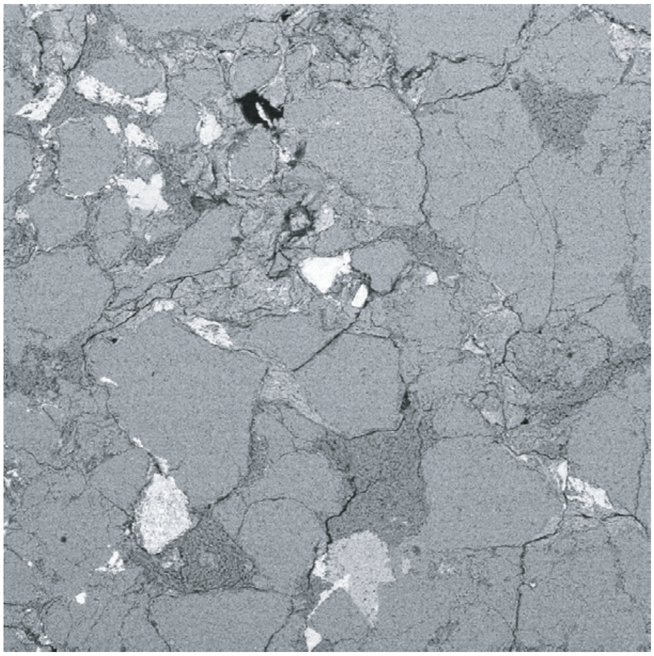

0.5 mm

1–2 mm zone of intense fracturing and granulation (Figs 3b and 3c). The boundaries of the pre-existing fault retain their primary form and are sharp. Little deformation is noted at distances of tens of microns outside this zone. Hairline fractures crosscut most framework grains within the reactivated fault zone and a number of large dilatant fractures (apertures of 10–50 μm) are present. These dilatant fractures run parallel to the original fault boundary and are acutely oriented (~30°) to the σ_1 direction (Fig. 3c). Fracturing resulting from reactivation has also resulted in a relatively consistent, sub-vertical fracture orientation sub-parallel to the σ_1 direction (Fig. 3b). These fractures are occasionally linked via subsidiary sub-horizontal fractures. Low angle shear displacement fractures appear to have originated at grain contact points resulting in patches of highly random fracture orientations. Fracturing is most intense along the cataclasite-reservoir boundary. These fractures are interpreted to form networks akin to a structural permeability mesh in which shear and tensile fractures form interlinked networks (Sibson, 1996). Fracturing is generally limited to the largest quartz and feldspar grains. Fine-grained quartz within the original cataclasite generally appears to be unfractured (Fig 3b).

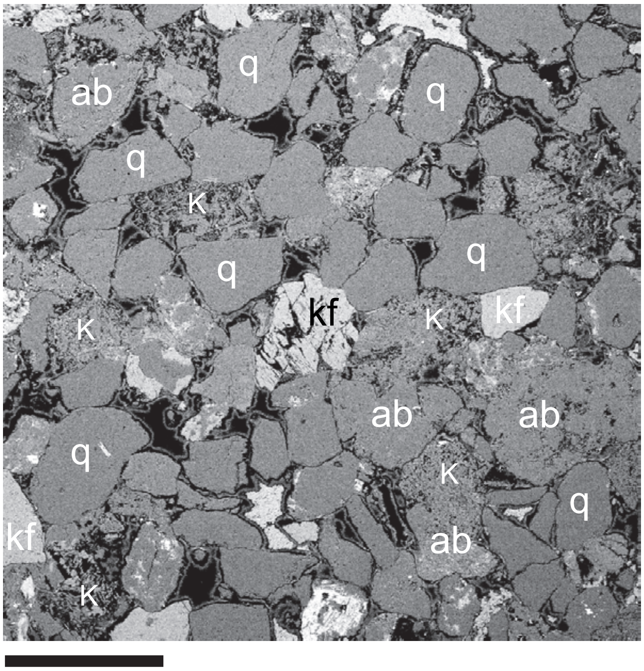

Figure 3a. Backscattered SEM image of a reservoir sandstone from Banyula–1 in the Otway Basin. Grains labelled are quartz (q), albite (ab), potassium feldspar (kf) and kaolinite (k). Pores are black and in many places are lined with chlorite which itself originally rimmed now dissolved grains. Feldspar dissolution, replacement by kaolinite and albitisation are evident. Embayed quartz grain contacts are indicative of solution transfer processes.

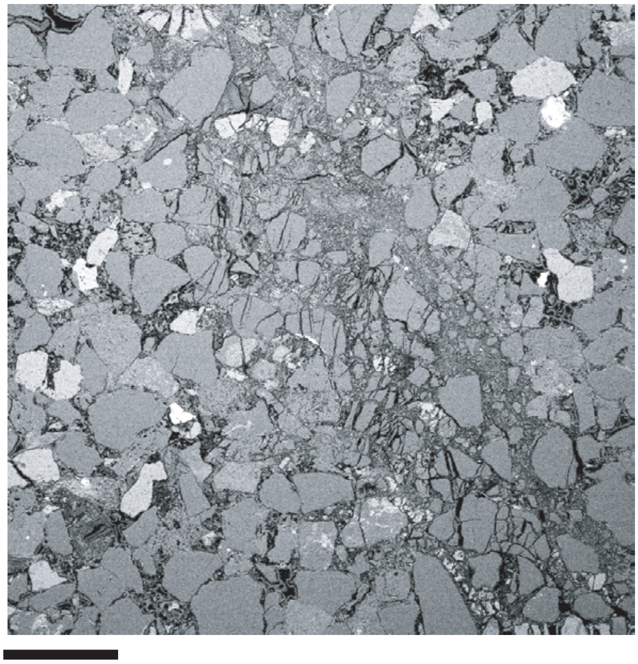

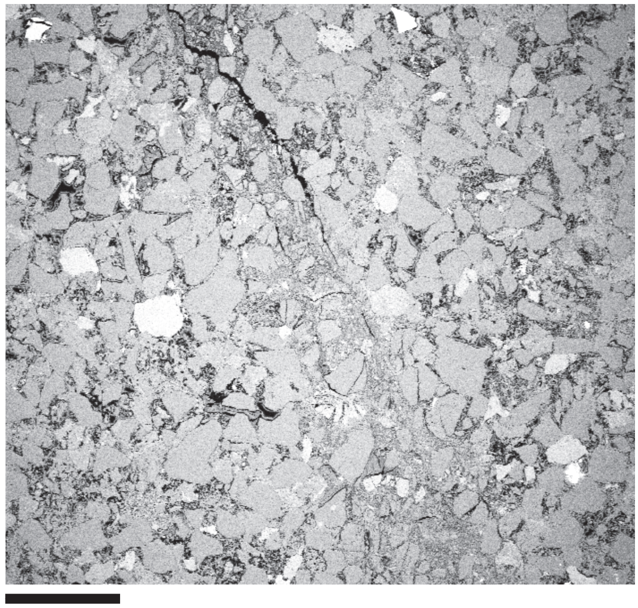

Figure 3b (top). Cataclasite microstructure from Banyula–1 after experimental reactivation. The initial cataclasite microstructure can still be seen comprising fine grained fractured grains and quartz cement. Tensile fractures are evident running along the cataclasite-reservoir boundary, which become mixed tensile and shear fractures towards the base of the image. Away from the reactivated zone, the reservoir sand is relatively unaffected by deformation.

Figure 3c (bottom). The same reactivated cataclasite as in (b) but further along the fault zone shows mainly evidence of deformation by shear fracturing.

Within the shear zone, the mode of failure changes from intense grain fracturing to a single through-going open fracture running initially along the base of the cataclasite-host rock contact (Figs 3b and 3c). Grain fracturing is absent around this open fracture. The lack of macro-fracture wall symmetry suggests that a small degree of shear has occurred during dilation. A small secondary open fracture set is apparent along the top of the cataclasite-host rock contact. This transition from discrete, large, open inter-grain fractures to intense granular fracturing is abrupt with the large open fracture terminating within an intensely fractured potassium feldspar grain. The framework quartz grains of the host sandstone beyond the shear zone are unaffected by experimental reactivation.

CARNARVON BASIN MICROSTRUCTURAL AND POROSIMETRY RESULTS

The Echo/Yodel gas condensate field (Fig. 4a) is located on the Rankin Trend in the Dampier sub-Basin. Upper Triassic fluvio-deltaic Mungaroo Formation sands form the primary reservoir unit and sub-crop the Main Unconformity (MU play level) within a northwesterly dipping tilted fault block. Cretaceous claystones of the Muderong and Forestier Claystone Formations form the regional seal providing a combined structural/ stratigraphic trap.

The fault intersected by Yodel–2 is visible on semblance data (Fig. 4b) and has a throw of ~10–15m. Coring of the reservoir intersected sub-seismic faults at a density indicative of inner damage zone architecture. Deformation features within the core are well-lithified and cemented, while the undeformed host reservoir, a medium to coarse-grained sandstone, is friable due to partial cementation by quartz and kaolinite (Fig. 5). Small faults (1–3 mm gouge width) are noted on both sides of the inner damage zone up to at least 15 m in distance (maximum core length) from the principal slip plane. The variation in sandstone grain size over the 30 m core length gives rise to varied microfault width and geometry. Where little variation occurs, microfaults are single strands of constant width. Where grain size has a larger range, fault traces tend to refract through the interface and are thinner where grain size is finer.

The reservoir sandstone is loosely cemented and friable in hand specimen. It is medium to coarse-grained and highly porous, comprising mainly quartz with subsidiary potassium feldspar as framework grains. Some of these framework grains are fractured and some variations in diagenetic features are noted among the reservoir rocks. In Figure 5b, many pores are lined with diagenetic kaolinite and fine-grained bright specks of pyrite. Most quartz grains are in point contact with one another although there is evidence for minor diffusive mass transfer and local cementation at some grain contacts. Potassium feldspar dissolution is also evident but little secondary porosity appears to be present. In other parts of the reservoir (Fig. 5c), quartz grains predominate, more grain fracturing is evident, less kaolinite and pyrite are present and there appears to be more influence of diffusive mass transfer at grain contacts. Grain morphology in this image is suggestive of quartz overgrowths into the pore space. Porosity is still high, with large well-connected pores evident.

The microstructure of the principal fault recovered by Yodel-2 core is complex and can be divided into two distinct domains.

1. Fault gouge is heavily cemented by pyrite and is composed of unfractured and cataclastic components. The presence of both fractured and unfractured framework grains suggests this fault rock lies on the protocataclasite-cataclasite classification boundary (Fisher and Knipe, 1998). Pyrite crystals range from large (mm) to dust-sized (mm) particles. It is unlikely that this fault could have acted as a conduit for fluid-flow for sufficient time to allow growth of large pyrite crystals, rather that secondary pyrite cementation occurred following deformation.
2. Domain 2 surrounds the pyritised fault gouge. Here cataclastic processes have reduced grain sizes and increased the efficiency of fault gouge grain packing. Significant diffusive mass transfer has resulted in

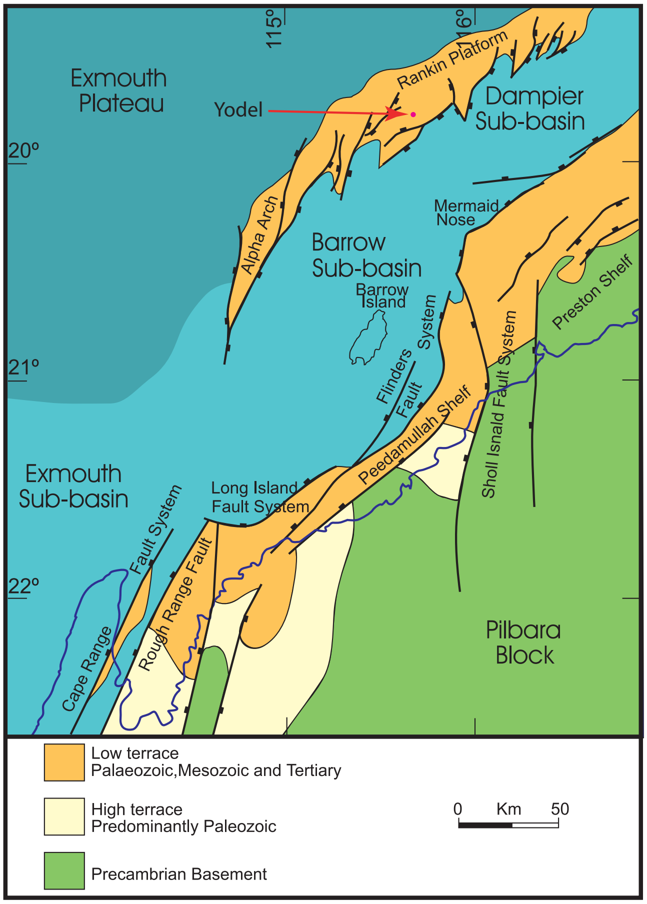

Figure 4 a. Location map showing the position of the Echo-Yodel field in the Carnarvon Basin.

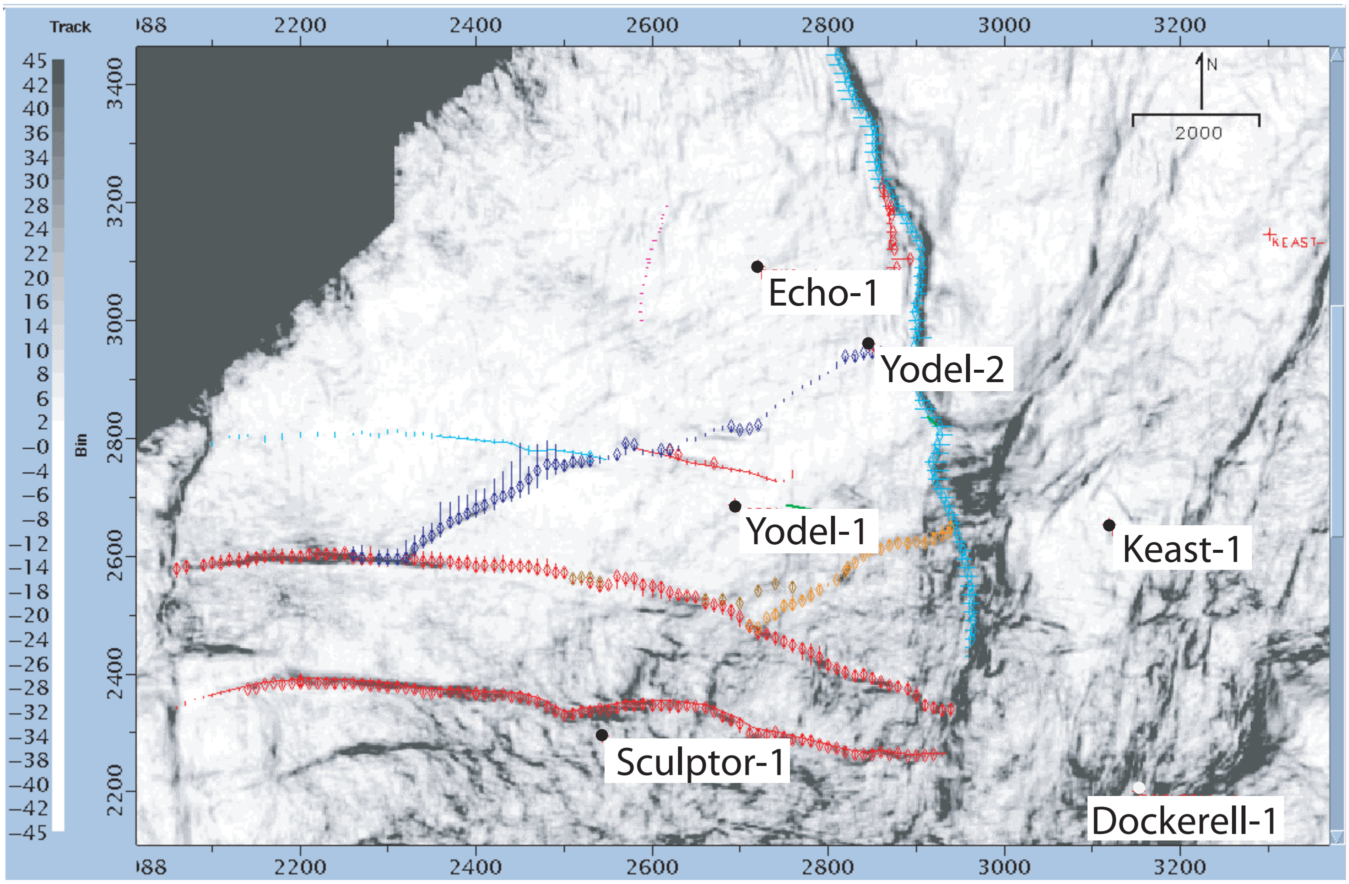

Figure 4b. Semblance time slice at top reservoir. Note location of fault in proximity to the Yodel–2 well position. Fault is highlighted in blue.

enhanced quartz cementation throughout this fault domain. Pore lining/occluding kaolinite is also present and has been deformed. Pyrite is confined to dilated fault strands, although occasional offshoots from microfaults are observed (Figs 5d and 5e). Little post cementation grain fracturing is noted.

Figure 5f shows a pyrite-cemented microfault from the outer damage zone of the main fault. The deformation features and morphology are remarkably similar to those observed in the multiple faults strands within the inner fault damage zone (Fig. 5d). The microfault is significantly dilated with whole quartz grains entrained and some minor cataclasis. Fracturing of pyrite also occurs within the microfault.

Microstructural analysis of these faults indicates that deformation occurred after kaolinite precipitation and dissolution of potassium feldspar. The faults are not heavily quartz cemented suggesting most fault activity occurred at shallow depths and temperatures <90ºC. However, cataclasis is observed and the wide grain-size distribution exhibited by these faults suggests more than one phase of deformation. Unfractured framework grains within the fault zones suggests deformation at low effective stresses and concomitant disaggregation. The degree of cataclasis is consistent with deformation at intermediate effective stress levels (10–20 MPa) at depths of 1–2 km (Menendez et al, 1996).

Capillary pressure measurements on faults in the outer damage zone from Yodel–2 show threshold pressures in the region of 40–80 psi, which, while higher than that of the reservoir (2–4 psi), will not form a significant seal over geological time. However, the inner fault damage zone has threshold pressures of ~8,500 psi and has a permeability to water (0.02 mD) six orders of magnitude lower than that of the undeformed reservoir sandstone (10 D). These data indicate significant seal capacity, and reflect more efficient grain packing and cementation within the principal fault zone. Hence, this inner zone probably represents a baffle on both geological and production timescales.

GEOMECHANICAL RESULTS

Cataclasites from Banyula–1 in the Otway Basin have lower cohesive strength (5.4 MPa) than the reservoir rocks (8.8 MPa; Fig. 6) but have a higher friction coefficient (0.78 as opposed to 0.67). The failure envelopes intersect at ~30 MPa, indicating in this case that the cataclasites are more likely to fail at low differential stress while the reservoir sandstone would fail at high differential stress. Jacaranda Ridge–1, reservoir

Figure 5a. Fault zone in core from Yodel–2 in the Carnarvon Basin. The fault zone is thick compared to typical microfaults seen in core and has accommodated around 15 m of slip in multiple episodes. The boundaries of the hard, cemented fault zone with the surrounding friable reservoir are sharp. This fault seals a hydrocarbon accumulation at the current day.

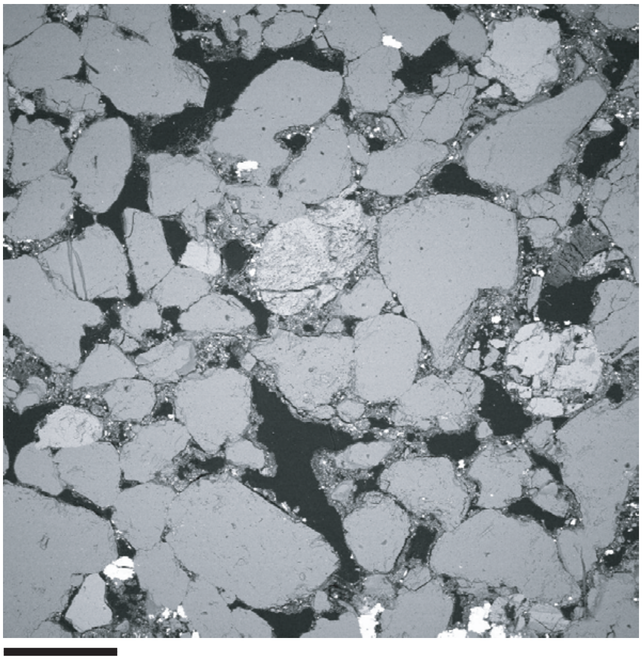

Figure 5b. Backscattered electron image of the Yodel–2 reservoir sandstone showing high, well connected porosity, with minor kaolinite and quartz cementation. Dark grains are quartz and lighter large grains are potassium feldspars.

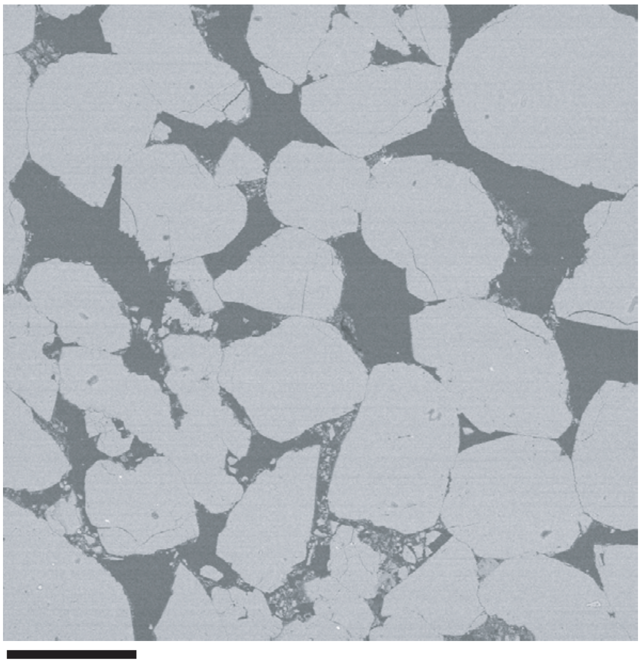

Figure 5c. Variability within the Yodel-2 reservoir sandstone, with little kaolinite cement and very high porosity. Some quartz overgrowths are evident.

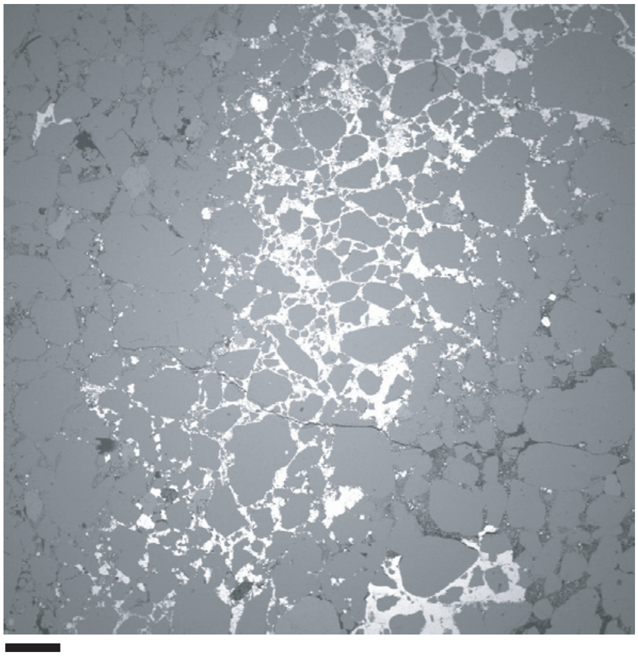

Figure 5d. Pyrite (bright) cemented protocataclastic microfault from the main fault in (a). Some fracturing of quartz is evident, although some grains are entrained into the fault zone whole. Kaolinite is also deformed indicating precipitation pre-deformation,

sandstones, cataclasites and phyllosilicate framework faults all have similar failure envelopes (Fig. 7). Fault cohesive strength ranges from 12.5–14.8 MPa and friction coefficients are 0.75–0.86. Surprisingly, the clay-rich fault rocks exhibit the greatest cohesive strengths, highest friction coefficient and are stronger than the cataclasite or reservoir rock at all effective normal stresses. The failure envelopes of the cataclasite and reservoir sandstone intersect at effective normal stresses of around 25 MPa, and suggest that the cataclasite is more likely to fail when differential stress is high, while the reservoir would preferentially fail under low differential stress conditions.

The principal fault from the Yodel–2 core exhibits cohesive strength of ~17 MPa and friction coefficient of 1.12, well in excess of the outer damage zone microfaults and reservoir rocks tested from this well (Fig. 8). Minor outer damage zone faults have failure envelopes that fall in a narrow band with cohesive strengths between 3.76–10.11 MPa and friction coefficients of 0.59–0.87. Hence the high strength of the core of the fault zone in this area is likely to govern the reactivation potential of this fault.

The importance of these geomechanical results is twofold. Firstly they demonstrate that fault rocks can have significant cohesive strength, which allows them to fail by tensile, shear or mixed mode mechanisms. Secondly, they show that while fault rocks can be weaker than their host reservoir sandstones, as is often assumed, they can also be appreciably stronger as a result of post

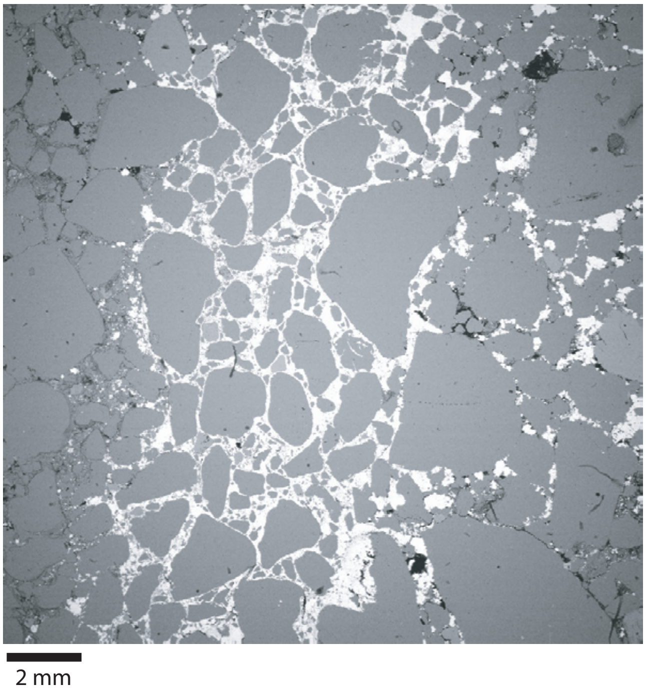

Figure 5e. Pyrite-cemented fault zone showing poor sorting of fractured grains indicative of multiple slip episodes along the fault plane.

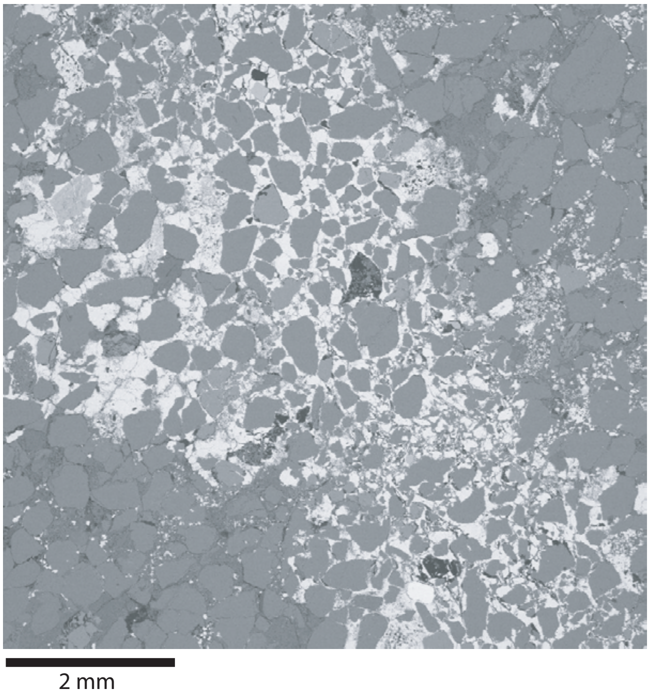

Figure 5f. Pyrite cemented fault zone from the damage zone around 10m from the major slip surface. These faults are strikingly similar in appearance to those in the major fault zone but have much lower threshold pressures.

deformation lithification/cementation. Both these observations have significant implications for the assessment of reactivation potential and associated seal breach through geomechanical methods. Current geomechanical methods for assessing reactivation potential often assume cohesionless fault planes and thus shear failure alone, not allowing for the development of tensile and mixed mode fractures. This may lead to a significant error in assessing reactivation potential and thus fault seal integrity. Equally importantly, most geomechanical analyses implicitly assume that fault rocks are weaker than the reservoir rocks from which they were derived, but the laboratory results and microstructural observations presented above show that this is not always the case. Where fault rocks are stronger than their host, different methods need to be employed to detect the properties of such faults. The two cases of stronger fault rocks presented here both intersect hydrocarbon columns and prevent vertical leakage from these pools.

PREDICTING THE RISK OF WEAK FAULT REACTIVATION

The likelihood of weak fault reactivation and associated seal breach can be assessed given knowledge of the stress field, fault orientation and the failure envelope for the fault rocks. Reactivation risk is assessed with respect to the in situ stress field that is determined by a variety of geomechanical techniques. Density and check shot velocity data yield the vertical stress; borehole breakouts and drilling-induced tensile fractures yield the orientation of the horizontal stresses; leak-off and extended leak-off tests yield the minimum horizontal stress; and the maximum horizontal stress is determined by the occurrence or non-occurrence of breakouts and drilling-induced tensile fractures and knowledge of rock strength (see Bell, 1990; 1996; Moos and Zoback, 1990; Hillis and Reynolds, 2000). Fault orientations (dip and dip direction) are determined from seismic interpretation, based on the offset between reflector terminations at a fault. Knowledge of the failure envelope is determined from laboratory testing of intact fault rocks as described above and constitutes a critical difference between the technique presented here and previous methods for assessing fault reactivation risk (Morris et al, 1996; Ferrill et al 1999; Wiprut and Zoback, 2000; Castillo et al, 2000).

Given the above information, there are three critical stages to assessing reactivation risk:

a) A 3D Mohr diagram representing the state-of-stress and failure envelope for the fault is constructed (Fig. 9). The risk of reactivation of a plane of any orientation is expressed by the increase in pore pressure (ΔPp) required to cause its reactivation, i.e. horizontal distance on a 3D Mohr diagram between a plane and the failure envelope.
b) The reactivation risk (ΔPp) for all planes is plotted on a poles to plane, lower hemisphere stereonet (Fig. 10).

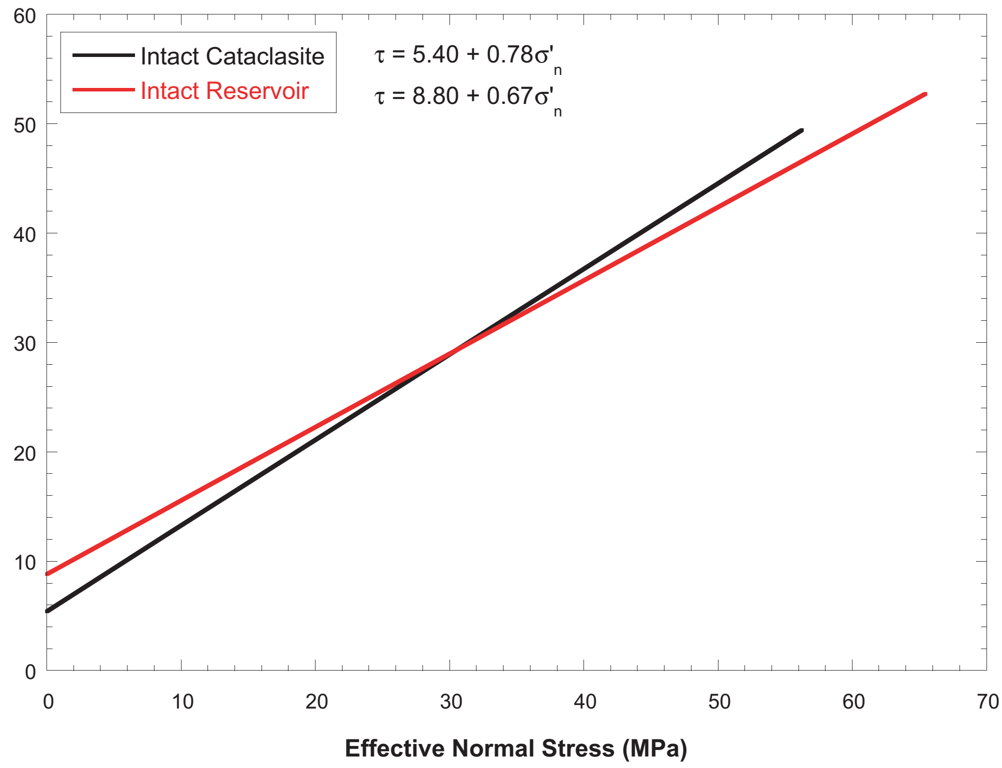

Figure 6. Failure envelopes for the cataclasite and host reservoir at Banyula–1. At low effective normal stress (<30 MPa), the cataclasite is weaker than the host reservoir sandstone. Friction coefficients fall in the range specified by Byerlee (1978) for sedimentary rocks under low stress conditions but the fault rock has developed significant cohesive strength (~5.4 MPa).

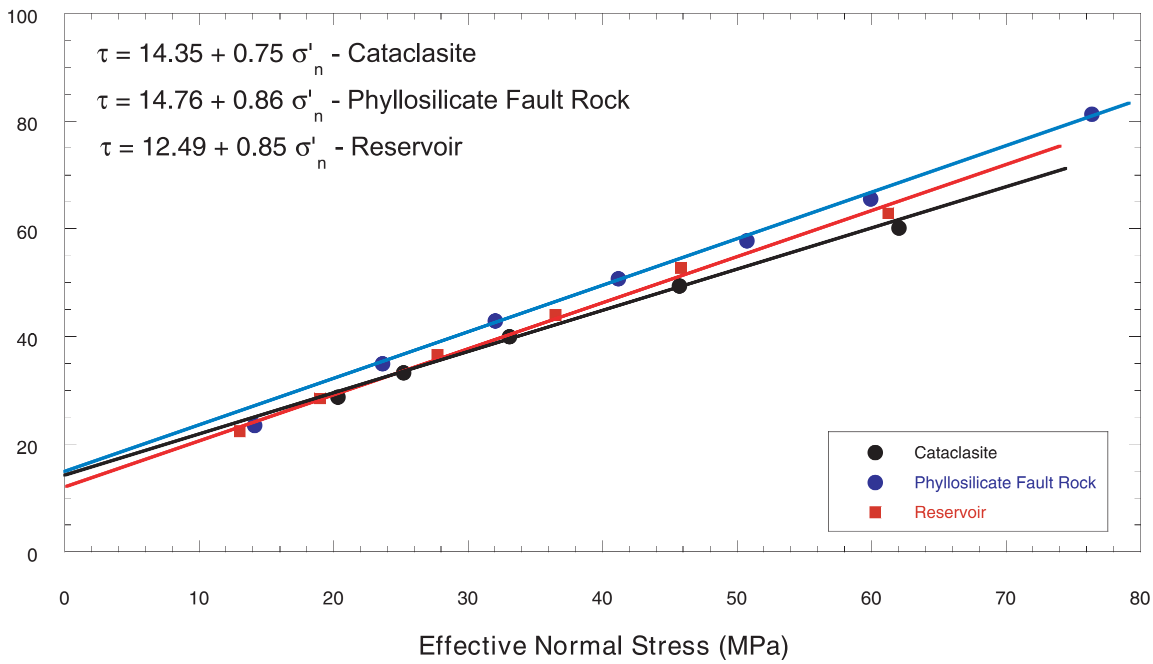

Figure 7. Failure envelopes for cataclasite, phyllosilicate framework fault rock and host sandstone from Jacaranda Ridge–1. Under all effective normal stress conditions, the phyllosilicate fault rock is the strongest rock and has high cohesive strength (~14.8 MPa). The host sandstone is weaker than the cataclasite at low effective normal stress (<25 MPa) but stronger above this level. The cataclasite also has appreciable cohesive strength (14.35 MPa).

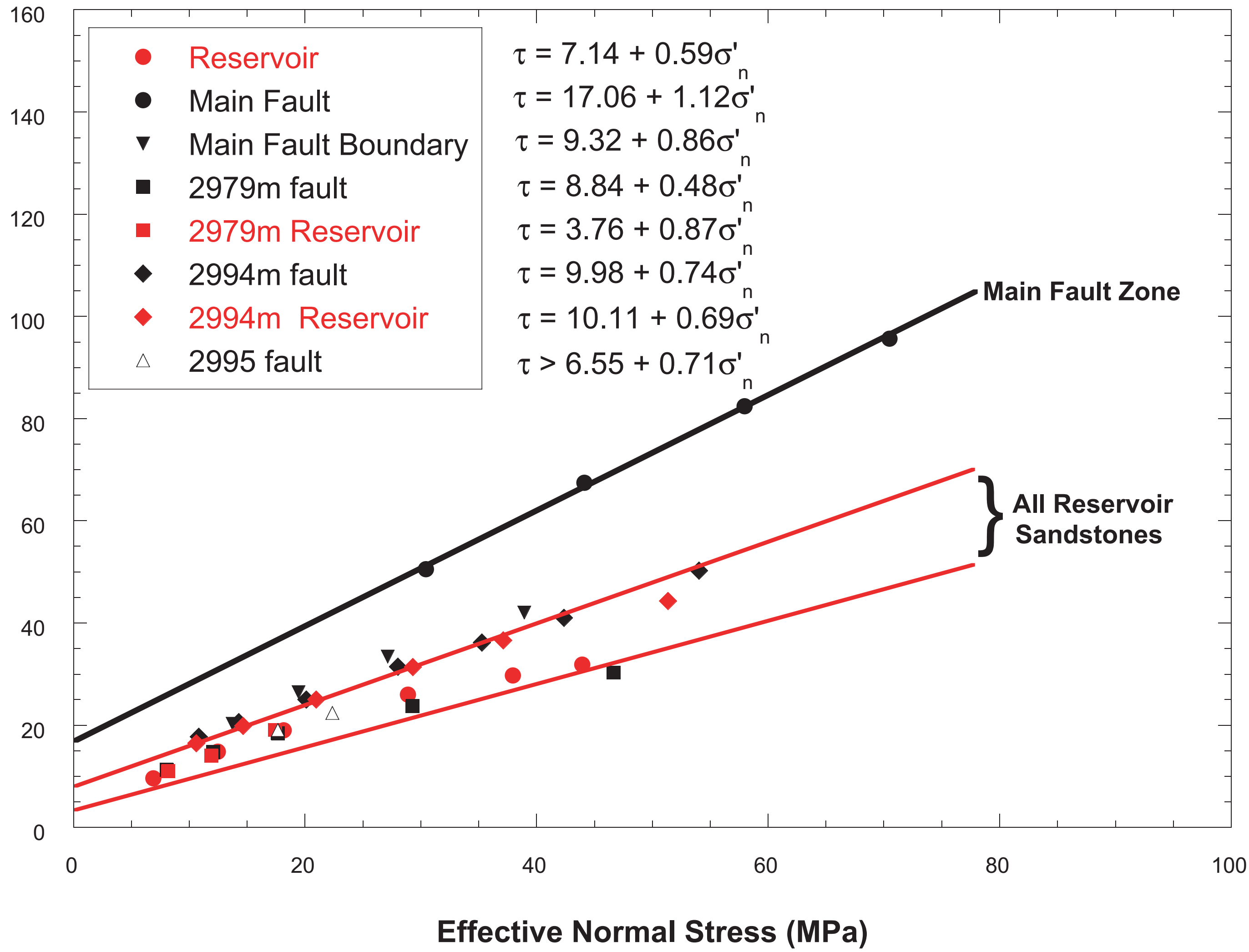

Figure 8. Failure envelopes for the main fault zone, the boundary between the main fault and reservoir, the reservoir itself and damage zone microfaults from Yodel–2. The main fault zone has a high cohesive strength (~17 MPa) due to intense quartz and pyrite cementation. The boundary between the fault and reservoir is also strong, although the reservoir away from the main fault, and the microfaults in the damage zone, have similar geomechanical properties.

c) Fault architecture is mapped and polygons are collapsed to a series of centreline points. Each point along the fault has an associated dip and dip direction. The reactivation risk (ΔPp) for each fault segment is subsequently mapped on to the fault centreline trace (Fig.11). These data incorporate 3D information in a 2D plane.

The advantages of this methodology are twofold. Realistic failure envelopes derived from laboratory tests can be considered with respect to the in-situ stress field and the likelihood of reactivation by all modes of failure can be assessed with a single calculation as opposed to the separate slip and dilation tendency analyses of Ferrill et al, (1999).

Otway Basin case study

The Zema–1 well in the Otway Basin, South Australia intersected an 86 m palaeo-gas column and a 15 m palaeo-oil leg in the Lower Cretaceous Pretty Hill Formation. The Zema structure required fault seal for an effective trap to be present and is bounded by a large east–west trending fault with a change in strike to northwest–southeast towards the eastern tip (Fig 11). Detailed analysis suggested that both juxtaposition and fault deformation processes were likely to provide an adequate seal for the observed palaeo-column (Jones et al, 2000). Hence the propensity for reactivation-related breach of the fault seal at Zema–1 was investigated.

The in situ stress regime at 2,860 m, the depth of the base of the regional seal, in the offset Katnook–3 well (for

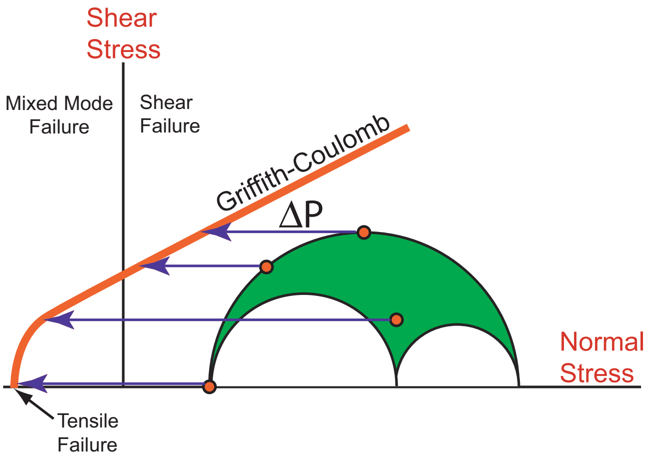

Figure 9. Three-dimensional Mohr diagram with composite Griffith-Coulomb failure envelope. All possible orientations of fault planes lie within the shaded area. The horizontal distance between a plane of any orientation and the failure envelope (which can be thought of as the increase in pore pressure (ΔPp) required to cause failure) is used to characterise the propensity of that plane to fail.

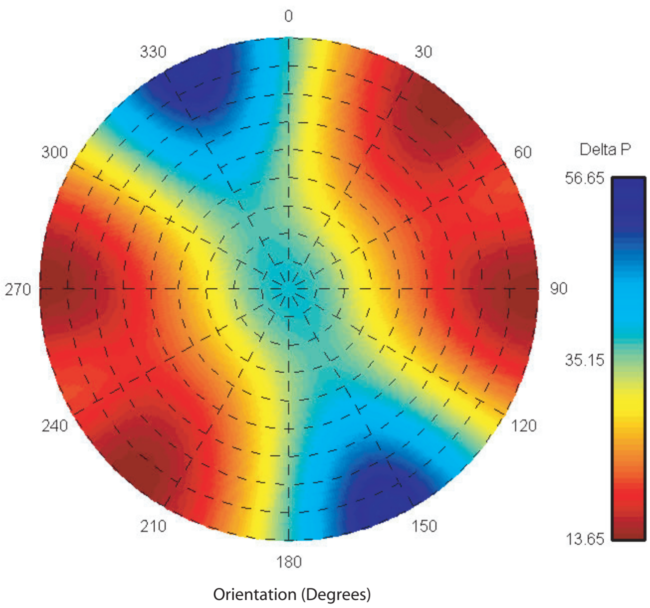

Figure 10. Likelihood of reactivation of fault/fracture planes in the Penola Trough, Otway Basin, based on the in situ stress regime and the failure envelope derived for the cataclasite in Banyula–1. Numerical values on the scale refer to ΔPp values. Equal angle, lower hemisphere stereographic projection of poles to planes.

which the requisite data to determine the in situ stress field were available) was taken to be representative of that in the Zema prospect. The techniques described above were used by Jones et al, (2000) to constrain the in situ stress field to:

Minimum horizontal stress (σ_h) = 46 MPa;
Overburden stress (σ_v) = 64 MPa;
Maximum horizontal stress (σ_H) = 82 MPa; and
Pore pressure (Pp) = 28 MPa,
Maximum horizontal stress (σ_H) orientation = 156°N.

The failure envelope used ($t = 5.4 + 0.78\sigma_n'$) is that derived for the intact cataclasite at Banyula–1 (Fig. 6), bearing in mind the assumption that geomechanical properties remain similar over the distance between these two wells (Fig.1).

The resultant polar plot and reactivation risk map (Figs 10 and 11) reveal that a section of the fault bounding the Zema prospect is prone to be reactivated within the in situ stress field. Given that juxtaposition and fault deformation processes are likely to have created an adequate seal, and that the trap-bounding fault is prone to reactivation, we interpret that fault reactivation is indeed primarily responsible for seal breach and thus the presence of the palaeo-column in the Zema–1 well. Microstructural analysis confirms the presence of open fractures in the subsurface associated with the cataclasite (Jones et al, 2000) and laboratory reactivation of the cataclasite showed the propensity for the development of an interlinked tensile and shear fracture network (Fig. 3b).

Also noteworthy here is that there is significant variation in reactivation risk along fault segments with relatively constant strike in the Otway Basin (Fig. 11). This is primarily a consequence of changing dip along the fault and indicates that the risk of fault reactivation must be considered as a 3D problem and cannot be assessed using fault strike data alone.

CONSIDERATION OF STRONG FAULTS

Strong faults are those that fail at higher shear stress than intact reservoir rocks for the same effective normal stress. The strength testing undertaken herein reveals several types of strong faults. The phyllosilicate framework fault rock at Jacaranda Ridge–1 (Fig. 7) and the main fault zone from Yodel–2 (Fig. 8) are stronger than their respective intact host reservoir sandstones at all effective normal stress levels. The cataclasite at Jacaranda Ridge–1 is stronger than the reservoir sandstone at low effective normal stress but becomes weaker at normal stresses >25 MPa (Fig. 7). The cataclasite at Banyula-1 is weaker than the intact reservoir rock at low effective normal stress but stronger at effective normal stresses > 30 MPa (Fig. 6).

Geomechanical techniques used to predict fault reactivation based on the assumption of zero cohesion are particularly inappropriate in the case of strong faults. Such strong faults are unlikely to be reactivated and the seal risk is consequently lower at these localities. At Yodel–2 and in the case of the phyllosilicate framework fault rock at Jacaranda Ridge–1, reservoir rocks would fail before fault rocks under all prevailing stress conditions. In these cases, the orientation of the trap-bounding fault is not relevant to assessing reactivation potential. The preservation of hydrocarbon columns at

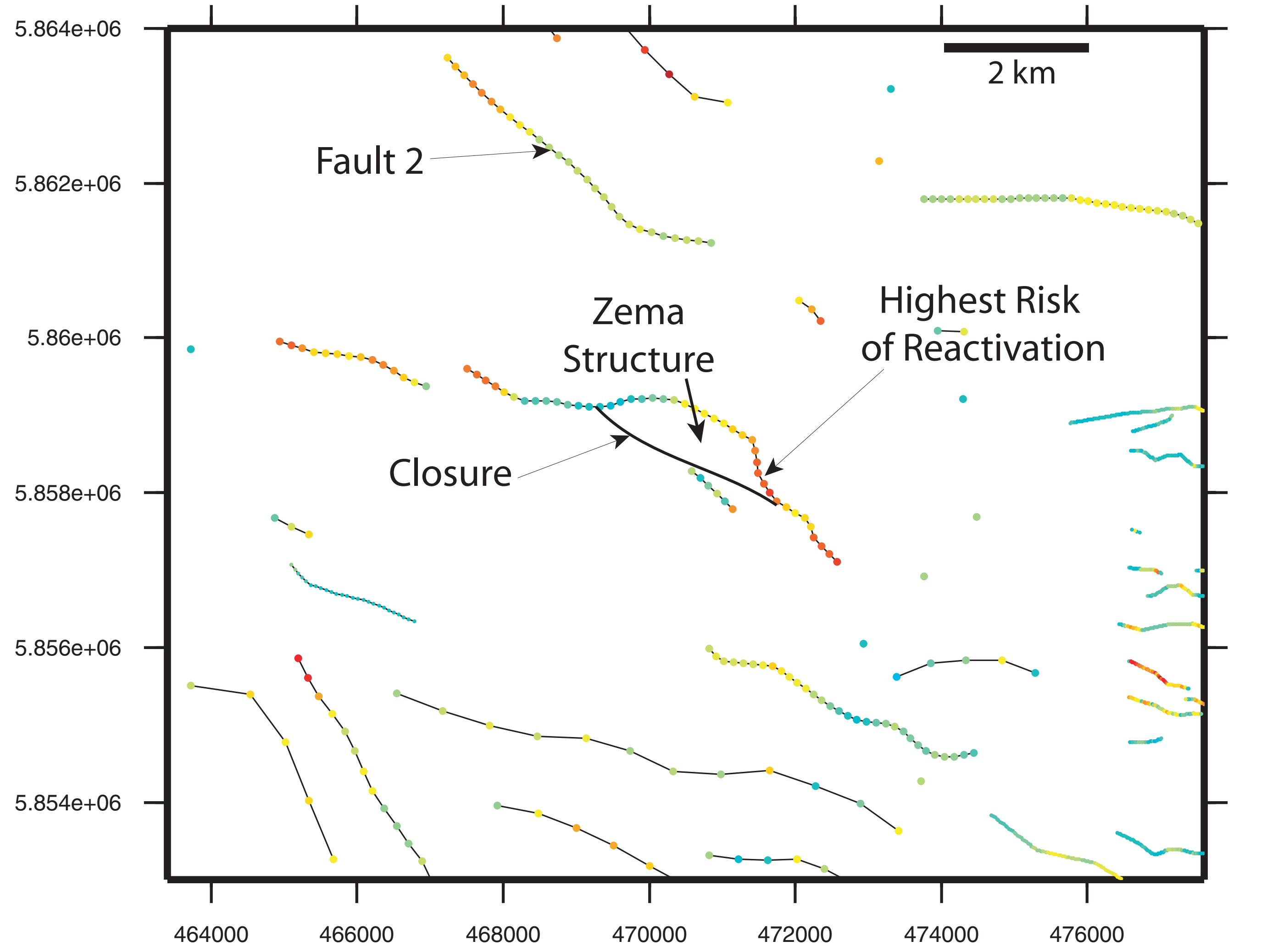

Figure 11. F.A.S.T. map of the likelihood of reactivation of fault/fracture patterns for the Zema prospect in the Penola Trough, which intersected a breached palaeocolumn. Colours along the fault segments refer to reactivation risk (ΔPp) values from Figure 10. The highest risk of reactivation (lowest ΔPp) coincides with the major fault closure on the structure. Variations in risk along the almost constant strike of Fault 2 are due to changes in fault dip.

these localities may be intimately related to the fact that the trap-bounding faults are strong and thus not prone to reactivation.

Future research on seal breach related to fault reactivation needs to focus not only on geomechanical techniques for predicting the likelihood of reactivation of weak faults, but also on the prediction of failure envelopes and whether trap-bounding faults are likely to be stronger than intact reservoir rock (using such data as burial and temperature history and rock composition). An additional complication in the case of strong fault rocks that needs to be considered is the likelihood of reactivation of the interface between fault and intact rock (Streit, 1999). The competency contrast at fault-reservoir boundaries has been observed microstructurally to play a role in cataclasite reactivation (Dewhurst and Jones, in press). Major faults can develop damage zones many tens of metres in extent and these latter areas may in fact be weaker than cemented fault cores. For example, the boundary between fault core and reservoir in Yodel-2 is weaker than the main fault zone, while damage zone microfaults and intact reservoir sandstones tend to have similar geomechanical properties (Fig. 8).

IMPLICATIONS

Faults can seal by a number of mechanisms including clay smear, cataclasis and cementation. Such processes are directly relevant to the strength of the fault rock products formed in that their ductility and/or lithification state will govern their geomechanical response. In the case of clay smear and cataclasis alone (i.e. without post deformation lithification), fault strength will be controlled by the residual strength of the fault rocks and in general, such deformation will be cohesionless, or nearly so. However, where significant cementation has taken place within fault cores and the more permeable damage zones, fault strength can increase and the results above show that that increase in strength can in fact be above that of the host reservoir lithology.

Sibson (1998) and Barton et al, (1995) have also demonstrated the contribution of optimally oriented shear fractures to structural permeability. For example, if differential stresses are high (greater than 6T, where T is tensile strength), Mohr's circle can only touch a failure envelope in positive effective normal stress space which results in the development of shear fractures. Similarly, if fault zones have zero cohesive strength, then the failure envelope passes through the origin of the Mohr construction and failure can only occur in shear fracture space, regardless of the magnitude of the differential stress.

The regeneration of fault rock strength through cementation can result in the development of considerable cohesive and therefore tensile strength thus allowing the possibility of more than one mode of failure. In describing the role shear failure plays in reactivated fault zones, Sibson (1996, 1998) also notes the conditions under which tensile and mixed mode fractures may play a role in the development of structural permeability networks. Where tensile strength exists, tensile failure can occur under low differential stress conditions (σ_1-σ_3<4T), while mixed mode extensional shear fractures form at differential stresses intermediate to tensile and shear failure (4T-6T) using a Griffith-Coulomb failure envelope. In general, many instances of fracture-induced top seal failure have been ascribed to tensile failure as a result of pore fluid pressure reducing minimum effective stress beneath that of rock tensile strength (e.g. Watts, 1987; Caillet, 1993). However, in fault zones, reactivation in tension can only occur when faults have become severely misoriented for shear reactivation with respect to the stress field or when such faults have regained cohesive strength due to cementation (Sibson, 1996, 1998). Little data are available on the geomechanical properties of petroleum-related fault rocks, although those presented above tend to suggest that such rocks are by no means cohesionless or weak and may be considerably stronger than the reservoir rocks in which they are located. Fournier (1996) has shown that where a fault has a finite cohesive strength that is less than that of the host reservoir rock, failure may occur in the fault core by tensile, shear or mixed mode fracturing. While geomechanical techniques that assess reactivation based on shear failure alone are not inherently incorrect, a methodology that does not account for regained fault strength, and thus the possibility of tensile failure, could result in an erroneous determination of potential seal risk and, indeed, errors in the determination of orientations of structures most prone to reactivation. Due to the lack of geomechanical data for petroleum-related fault rocks, failure envelopes for fault reactivation are often estimated from data collated by Byerlee (1978), resulting in friction coefficients on the order of 0.60–0.85 and zero cohesive strength. The use of such assumed failure envelopes however only allows for shear failure conditions to develop as cohesive strength is zero. Closer examination of the data and theory presented by Byerlee (1978) shows that while an approximation that ignores cohesive strength makes little difference at high effective normal stresses (>100 MPa), the lower the effective normal stress, the greater the error induced by neglecting cohesive strength. It is likely that fault rocks in petroleum systems at depths of 1–4 km fall in the lower stress range where such errors can be significant. The existence of these errors was noted in Byerlee's (1978) paper to result from definitions of friction in that typically a linear relationship is assumed between shear stress and effective normal stress, such that:

$$\tau = C + B\sigma_n'$$

where τ is shear stress, C is cohesive strength, is effective normal stress and B is a constant often defined as the coefficient of friction (μ). However, the generally accepted definition of friction (Byerlee, 1978) is:

$$\mu = B + \frac{C}{\sigma_n'}$$

Hence, at shallow crustal levels in sedimentary basins, errors in geomechanical assessments of fault seal are contained not only in the assumption of zero cohesive strength and thus shear failure alone, but also in the definition of the friction coefficients themselves. Further to this, many of the data collated by Byerlee (1978) come from sawcuts in rocks, some of which were infilled with gouge material, which may not be representative of natural fault zones and thus geomechanical behaviour in the field. The presence of extremely strong fault rocks in the Carnarvon and Otway examples is testament to this. Where limited data are available for conducting geomechanical analysis of fault seal, it is recommended that sensitivity analyses be undertaken to determine the effects of both varying friction angle and increased cohesive strength along fault zones where seal breach due to reactivation is perceived as the major risk to the prospect.

In two of the fields described above, fault rock strength is greater than that of the reservoir, suggesting that deformation associated with reactivation would preferentially be partitioned into the weaker reservoir sediments. Hydrocarbon columns are associated with the fault zones from where these strong fault rocks were sourced. Current geomechanical predictive techniques that assume fault rocks are weaker than reservoir rocks assess seal risk based on orientation and dip and thus cannot account for situations where faults are the strongest link in an individual prospect.

CONCLUSIONS

The geomechanical properties of fault rocks govern their response to imposed stress fields and therefore significantly affect fault zone strength and reactivation potential. Fault rocks taken from the Carnarvon and Otway basins show significant post-deformation lithification due to quartz and/or pyrite cementation that has resulted in the regaining of cohesive and therefore tensile strength. Such fault healing allows the development of tensile, shear and mixed mode fractures which link together to form structural permeability networks. Microstructural observations from reactivated Otway Basin cataclasites show that both tensile and shear fractures can form in cemented cataclasites and can form effective conduits for fluid transfer.

Evaluation of seal risk in reactivated terrains can be undertaken using a geomechanical approach. Current techniques tend to assume faults are cohesionless and apply a simple friction law to derive a failure envelope, an approach which, while not inherently incorrect, may lead to errors in both orientations of faults at risk of reactivation as well as absolute degree of risk. Application of a new technique incorporating in situ stress conditions with laboratory derived failure envelopes in the Otway Basin fully corroborated seal breach in the Zema structure due to reactivation. In this area, where fault rocks are weaker than the surrounding reservoir sandstones, a geomechanical approach to seal risking is applicable. However, in two cases from the Carnarvon and Otway Basins, fault rocks were found to be stronger than the surrounding reservoir rocks due to preferential cementation. In such cases, the assumption of fault rocks being weaker than their hosts is not valid and therefore such an approach would incorrectly appraise the degree of reactivation risk.

ACKNOWLEDGEMENTS

This work was performed under the aegis of the Australian Petroleum Cooperative Research Centre (APCRC) program on Hydrocarbon Sealing Potential of Faults and Cap Rocks. Data and samples for the study were kindly provided by Woodside Energy and Origin Energy. The sponsors of this APCRC program (Woodside Energy, Origin Energy, OMV, JNOC, Globex, Santos, Exxon/Mobil, BHP, Chevron, Phillips) are thanked for their financial support and permission to publish. Ric Daniel at the National Centre for Petroleum Geology and Geophysics carried out the capillary pressure measurements. SEM work benefitted from the advice and preparation work of Colin MacRae and Cameron Davidson of CSIRO Minerals Division. Thanks are also due to Ed Kopsen and another reviewer for their thorough and constructive comments.

REFERENCES

AYDIN, A., 1978—Small faults formed as deformation bands in sandstone. Pure and Applied Geophysics, 116, 913–30.

AYDIN, A., AND JOHNSON, A.M., 1983—Analysis of faulting in porous sandstones. Journal of Structural Geology, 5, 19–31.

BARTON, C.A., ZOBACK, M.D. AND MOOS, D., 1995—Fluid flow along potentially active faults in crystalline rock, Geology, 23, 683–686.

BELL, J.S., 1990—The stress regime of the Scotian Shelf offshore eastern Canada to 6 kilometers depth and implications for rock mechanics and hydrocarbon migration. In: Maury, V. and Fourmaintraux, D. (eds), Rock at Great Depth, 3, 1,243–65.

BELL, J.S., 1996—In situ stresses in sedimentary rocks (part 1): measurement techniques, Geoscience Canada, 23, 85–100.

BYERLEE, J.D., 1978—Friction of rocks. Pure and Applied Geophysics, 116, 615–26.

CAILLET, G., 1993—The caprock of the Snorre Field, Norway: a possible leakage by hydraulic fracturing, Marine and Petroleum Geology, 10, 42–50.

CASTILLO, D.A., BISHOP, D.J., DONALDSON, I., KUEK, D., DE RUIG, M.J., TRUPP, M. AND SCHUSTER, M.W., 2000—Trap integrity in the Laminaria High-Nancar Trough region, Timor Sea: prediction of fault seal failure. APPEA Journal, 40 (1), 151–173.

CHESTER, F.M., AND LOGAN, J.M., 1986—Implications for mechanical properties of brittle faults from observations of the Punchbowl fault zone, California. Pure and Applied Geophysics, 124, 79–106.

DEER, W.A., HOWIE, R.A. AND ZUSSMAN, J., 1966—An introduction to the rock-forming minerals. Longman, UK, 528 pp.

DEWHURST, D.N., AND JONES, R.M., in press—Geomechanical, microstructural and petrophysical evolution in experimentally reactivated cataclasites: applications to fault seal prediction, AAPG Bulletin.

FERRILL, D.A., WINTERLE, J., WITTMEYER, G., SIMS, D., COLTON, S., ARMSTRONG, A. AND MORRIS, A.P., 1999—Stressed rock strains groundwater at Yucca Mountain, Nevada, GSA Today, 9, 1–8.

FISHER, Q.J., AND KNIPE, R.J., 1998—Fault sealing processes in siliclastic sediments. In: Jones, G., Fisher, Q.J., and Knipe, R.J., (eds), Faulting, fault sealing and fluid flow in hydrocarbon reservoirs. GSL, Special Publication, 147, 117–34.

FJÆR E., HOLT, R.M., HORSRUD, P., RAAEN, A.M., RISNES, R., 1992—Petroleum Related Rock Mechanics. Developments in Petroleum Science, 33, Elsevier, Amsterdam, 338 pp.

FOURNIER, R.O., 1996—Compressive and tensile failure at high fluid pressure where pre-existing fractures have cohesive strength, with application to the San Andreas Fault. Journal of Geophysical Research, 101/B11, 25,499–509.

GIBSON, R.G., 1998—Physical character and fluid flow properties of sandstone-derived fault zones. In: Coward, M.P., Daltaban, T.S., Johnson, H., (eds), Structural geology in reservoir characterization, GSL, Special Publication, 127, 83–97.

HILLIS, R.R. AND REYNOLDS, S.D., 2000—The Australian stress map, GSL Journal, 157, 915–21.

HIPPLER, S. J., 1997—Microstructures and diagenesis in North Sea fault zones; implications for fault-seal potential and fault-migration rates. In: Surdam, R.C., (ed), Seals, traps, and the petroleum system, AAPG Memoir, 67, 103–13.

JONES, R.M., BOULT, P., HILLIS, R.R., MILDREN, S.D., AND KALDI, J., 2000—Integrated hydrocarbon seal evaluation in the Penola Trough, Otway Basin. APPEA Journal, 40 (1), 194–212.

KOPSEN, E., SCHOLEFIELD, T., 1990—Prospectivity of the Otway Supergroup in the central and western Otway Basin. APEA Journal, 30 (1), 263–79,

LOVIBOND, R., SUTTILL, R.J., SKINNER, J.E., ABURAS, A.N., 1995—The hydrocarbon potential of the Penola Trough, Otway Basin. APPEA Journal, 35, 358–71.

MENÉNDEZ, B., ZHU, W., AND WONG, T-F., 1996—Micromechanics of brittle faulting and cataclastic flow in Berea sandstone. Journal of Structural Geology, 18, 1–16.

MOOS, D. AND ZOBACK, M.D., 1990—Utilization of observations of well bore failure to constrain the orientation and magnitude of crustal stresses; application to, Journal of Geophysical Research, 95, 9305–25.

MORRIS, A., FERRILL, D.A. AND HENDERSON, D.B, 1996—Slip-tendency analysis and fault reactivation, Geology 24, 275–278.

MORROW C.A., SHI L.Q., BYERLEE J.D. 1982—Strain hardening of clay-rich fault gouges. Journal of Geophysical Research, 87, 6,771–80.

MUIR WOOD, R., 1994—Earthquakes, strain cycling and the mobilization of fluids. In: Parnell, J. (ed) Geofluids: origin, migration and evolution of fluids in sedimentary basins, Geological Society Special Publication, 78, 85–98.

SCHOWALTER, T.T., 1979—Mechanisms of secondary hydrocarbon migration and entrapment, AAPG Bulletin, 63, 723–760.

SIBSON, R.H., 1992—Implications of fault valve behaviour for rupture nucleation and recurrence. Tectonophysics, 211, 283–93.

SIBSON, R.H., 1994—Crustal stress, faulting and fluid flow. In: Parnell, J. (ed) Geofluids: origin, migration and evolution of fluids in sedimentary basins, Geological Society Special Publication, 78, 69–84.

SIBSON, R.H., 1996—Structural permeability of fluid-driven fault fracture meshes. Journal of Structural Geology, 18, 1,031–42.

SIBSON, R.H., 1998—Conditions for rapid large-volume flow, in Arehart, G.B. and Hulston, J.R. (eds), Water-Rock Interaction: Proceedings, 9th International Symposium, 35–38.

STREIT, J.E., 1999—Conditions for earthquake surface rupture along the San Andreas fault system, California. Journal of Geophysical Research, 104, 17,929–39.

SVERDRUP, E., AND BYØRLYKKE, K., 1997—Fault properties and the development of cemented faulted zones in sedimentary basins: field examples and predictive models. In: Hydrocarbon seals: importance for exploration and production, Møller-Pedersen, P., and Koestler, A.G., (eds), Norwegian Petroleum Society (NPF), Special Publication, 7, 91–106.

WATTS, N. L., 1987—Theoretical aspects of cap rock and fault seals for two-phase hydrocarbon columns. Marine and Petroleum Geology, 4, 274–307.

WILLINK, R.J. AND LOVIBOND, R., 2001—Technology, teamwork, respect and persistence: ingredients of successful exploration in the onshore Otway Basin. APPEA Journal, 41 (1), 53–70.

WIPRUT, D. AND ZOBACK, M.D., 2000—Fault reactivation and fluid flow along a previously dormant normal fault in the northern North Sea. Geology, 28, 595–8.

APPEA

Authors' biographies over page.

THE AUTHORS

Dave Dewhurst obtained a BSc (Hons) in Geology from the University of Sheffield in 1987 and a PhD from the University of Newcastle Upon Tyne in 1991. Postdoctoral work at the University of Birmingham, the University of Newcastle Upon Tyne and Institut Français du Pétrole together with a three year stint at Imperial College, London, focussed on compaction, faulting and fluid flow in mudrocks. He joined CSIRO Petroleum in 1998 and is responsible for geomechanical, geophysical and petrophysical inputs to projects involving both overpressure prediction and cap/fault seal potential. Member: AAPG, GSL, AGU and PESA.

Richard Jones graduated in 1991 with Joint BSc (Hons) and PhD in 1995 from the University of Keele, England. After positions at GeoChem and Rock Deformation Research, Richard joined NCPGG in 1999 as Fault Seals Project Leader for the APCRC and industry sponsored Hydrocarbon Sealing Potential of Faults and Cap Rocks. He is now an Exploration Geologist working for Woodside Energy. He has worked extensively in the area of fault and top seal evaluation and has been involved with seals research programs in Europe, USA and Australia. Current interests include structural/seal evaluation and wellbore stability. Member: AAPG, PESA, PESGB.

Richard Hillis holds the State of South Australia Chair in Petroleum Reservoir Properties/ Petrophysics at the National Centre for Petroleum Geology and Geophysics (NCPGG), Adelaide University. He graduated BSc (Hons) from Imperial College (London, 1985), and PhD from the University of Edinburgh (1989). After seven years at Adelaide University's Department of Geology and Geophysics, Richard joined the NCPGG in 1999. His main research interests are in petroleum geomechanics and sedimentary basin tectonics. He has published approximately 50 papers, and has consulted to many Australian and international oil companies on these topics. Member: AAPG, AGU, ASEG, EAGE, GSA, GSL, PESA and SEG.

Scott Mildren is a research fellow at the National Centre for Petroleum Geology and Geophysics. He completed his PhD at the University of Adelaide in 1997 and took up a position as structural geologist with Z&S (Asia) Ltd. (now Baker Atlas Geoscience). At Z&S he interpreted resistivity and acoustic image data with application to in situ stresses and fracture characterisation. His current research addresses various petroleum related geomechanical issues such as fault seal integrity, fractured reservoirs and wellbore stability. Member: AAPG, ASEG, PESA and SPE.